Molecular Catalysis 509 (2021) 111578

Contents lists available at ScienceDirect

Molecular Catalysis

journal homepage: www.journals.elsevier.com/molecular-catalysis

Deracemization of diastereomerically pure *syn*- and *anti*-α-substituted β-hydroxyesters by Novozyme 435 lipase and determination of their absolute configuration by NMR spectroscopy

Christian Trapp [a,b,*], Kateřina Barková [a], Marek Jan Pecyna [a], Corinna Herrmann [a], Annett Fuchs [a], Dieter Greif [a], Martin Hofrichter [b]

[a] University of Applied Science Zittau/Goerlitz, Theodor-Körner-Allee 16, Zittau 02763, Germany
[b] TU Dresden, International Institute Zittau, Markt 23, Zittau 02763, Germany

ARTICLE INFO

Keywords:
Candida antarctica Lipase B
Novozyme 435
β-Hydroxyesters
Enzymatic kinetic resolution
NMR Spectroscopy
Catalysis
Molecular docking
Mosher's reagent

ABSTRACT

Enantiomerically pure α-substituted β-hydroxyesters are important chiral building blocks for ligands, auxiliaries and β-lactam antibiotics. A two-step chemo-enzymatic procedure using lipase as biocatalyst is an efficient way to synthesize such products. To date, the methods described are limited to molecules that do not contain a chiral center adjacent to the racemic carbinol, and furthermore, they are limited to acylation. Here, we investigated the deracemization of diastereomerically pure *syn*- and *anti*-α-substituted β-hydroxyesters containing two stereo centers, using experimental methods under neat conditions and classical molecule dynamics (MD) simulation. A screening of free and immobilized commercial lipases identified immobilized lipase B from *Candida antarctica* (Novozyme 435) as the most appropriate biocatalyst for sterically demanding α-substituted β-hydroxyesters. Using Novozyme 435, reaction conditions were optimized and hydroxyesters (*3S*) or (*3R*) were achieved with enantiomeric excesses up to ≥99% *ee* and maximum overall yields of 80%. The absolute configuration of the enantiomers was eventually determined by ^{1}H-NMR spectroscopy after derivatization with Mosher's reagent (α-methoxy-α-trifluoromethylphenylacetic acid = MTPA).

1. Introduction

Chiral β-hydroxyesters and α-substituted β-hydroxyesters represent versatile building blocks, which can be used for the synthesis of auxiliaries [1] (e.g. 1,2- or 1,3-amino alcohols [4]), β-lactam antibiotics [2] and pheromones [3]. They can be prepared biochemically or chemically. Biochemical routes proceed via reduction with isolated enzymes [5] or biotransformation with whole cells [6]. Main drawbacks of these approaches are insufficient solubility of nonpolar substrates in aqueous solvents and poor stabilities of most enzymes in pure organic solvents (neat conditions) [7]. Chemical methods to obtain these chiral hydroxyesters use aldol-type reactions [8] or asymmetric hydrogenation [9]. Furthermore, suitable combinations of chemical and enzymatic steps (chemoenzymatic approaches) turned out to be appropriate reaction setups. The latter start with Lewis acid-mediated diastereoselective reduction of analogous β-ketoesters using complexing and non-complexing metal salts like zinc [10], titanium [11] or cerium [11]. Afterwards, chiral resolution of these pure diastereomers can be achieved with lipases as enantioselective biocatalysts [12]. Notably, such combined approaches are working without platinum metals (e.g. ruthenium or iridium) unlike asymmetric hydrogenations [13].

Meanwhile the use of lipases as catalysts in organic synthesis has led to reliable synthetic routes that yield environmentally friendly products with high stereo- and regioselectivities [14]. One of the most important commercial lipases in organic synthesis is lipase B of the yeast *Candida antarctica* (CALB). It is typically used in immobilized form on macroporous poly(methyl methacrylate) resin and commercially available under the trade name Novozyme 435 (N435). The application of N435 has increased over the last two decades and includes reactions such as transesterification, Michael addition and epoxidation under mild and at the same time selective conditions [15]. One example is the N435 catalyzed resolution of racemic proxyphylline, a cardiac stimulant, vasodilator and bronchodilator, with a yield of 43% and *ee* up to >99% (E = 90) at a 5-g scale [29]. A second example is the resolution of racemic 1,2-propanediol using a packed-bed reactor filled with N435 to obtain (*R*)-propanediol with an E-value of >200 [38]. The usage of N435

* Corresponding author.
E-mail address: christian.trapp@hszg.de (C. Trapp).

https://doi.org/10.1016/j.mcat.2021.111578
Received 13 December 2020; Received in revised form 10 April 2021; Accepted 13 April 2021
Available online 23 May 2021

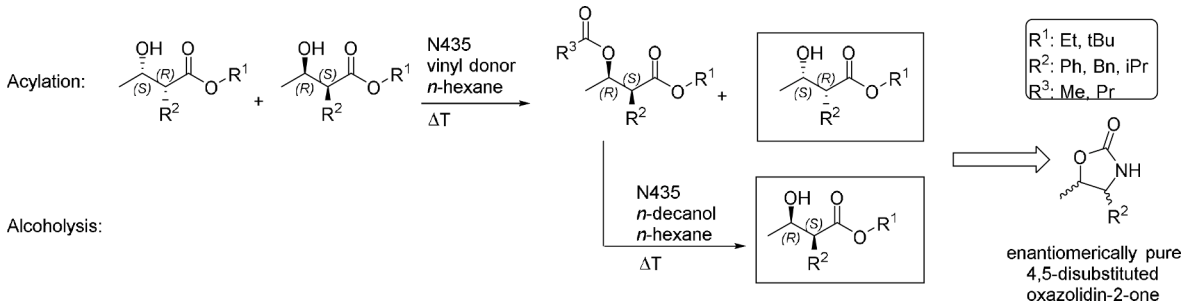

Fig. 1. Lipase-catalyzed kinetic resolution of α-substituted β-hydroxyesters in two steps. The formula scheme shows the resolution of *syn*-isomers as an example.

Table 1
Diastereoselective reduction of α-substituted β-ketoesters into the corresponding *syn*- or *anti*-β-hydroxyesters.

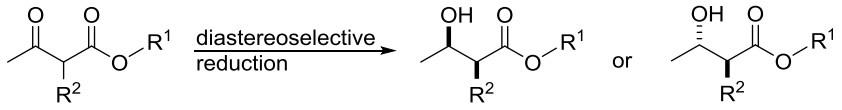

			syn-isomers **1-3**		*anti*-isomers **4-6**
syn-Hydroxyester	R^1	R^2	*anti*-Hydroxyester	R^1	R^2
1	Et	Ph	**2**	Et	Ph
3	Et	Bn	**4**	*t*Bu	Bn
5	Et	iPr	**6**	*t*Bu	iPr

in organic solvents is particularly relevant when reactants are poorly soluble in water or when reversal of the hydrolysis reaction is desired. However, the use of N435 is not limited to organic solvents; other reaction media such as ionic liquids [16], supercritical fluids [17] or deep eutectic solvents can be applied as well [18].

The resolution of racemic ethyl 3-hydroxybutanoate was already described for the preparation of enantiomerically pure (*3R*)- and (*3S*)-ethyl-3-hydroxybutanoate by *Fishman* et al.; they used vinyl acetate as acylating agent and lipase B from *Candida antarctica* in a solvent-free system giving 96% *ee* and 73% total yield [19]. Here, we were aiming at extending this elegant kinetic resolution on bulky 3-hydroxybutanoates with sterically hindered α-substituents (i.e. phenyl-, isopropyl- or benzyl-groups as ethyl or *tert*-butyl esters). For this approach, lipases were used as regio- and enantioselective biocatalysts to obtain the (*3S*)- and (*3R*)-hydroxyesters shown in Fig. 1. Afterwards, each pure enantiomer was used for the synthesis of chiral 4,5-disubstitued oxazolidin-2-ones.

Starting material of the aforementioned lipase reactions was synthesized by diastereoselective reduction of the corresponding β-ketoesters.

syn-Selective reduction followed Cram's chelate model, therefore coordinating Lewis acids, i.e. zinc and titanium salts, were used. The *anti*-selective reduction, however, followed the model according to Felkin and Anh. In this case, a sterically hindered reducing agent (lithium triethyl-borohydride, $LiEt_3BH$) and a non-complexing Lewis acid (cerium chloride, $CeCl_3$) were chosen as reactants. The pure diastereomers obtained were used for screening four lipases (free or immobilized enzymes), whereat we had a closer look onto the influence of *(i)* the type of α-substituent, *(ii)* the absolute configuration in α-position and *(iii)* the ester group (ethyl or *tert*-butyl ester) with regard to reaction rate and enantioselectivity. Eventually, we identified a suitable acyl donor for esterification and an adequate nucleophile for alcoholysis of the latter in different organic solvents.

Table 2
Acylation of *syn*- and *anti*-β-hydroxyesters[1] into the corresponding acyloxyesters.

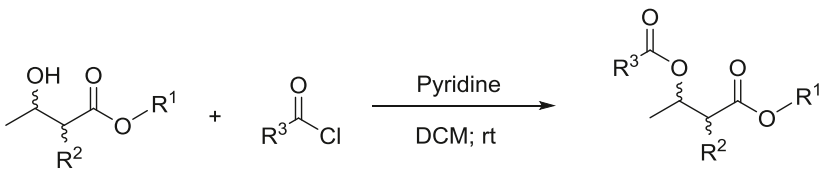

			1-6			**7-12**	
Hydroxyester	R^1	R^2	Acyloxyester	R^1	R^2	R^3	Yield
***syn*-1**	Et	Ph	***syn*-7**	Et	Ph	Pr	95%
***anti*-2**	Et	Ph	***anti*-8**	Et	Ph	Pr	95%
***syn*-3**	Et	Bn	***syn*-9**	Et	Bn	Pr	88%
***anti*-4**	*t*Bu	Bn	***anti*-10**	*t*Bu	Bn	Pr	95%
***syn*-5**	Et	iPr	***syn*-11**	Et	iPr	Me	88%
***anti*-6**	*t*Bu	iPr	***anti*-12**	*t*Bu	iPr	Pr	77%

[1] Only those acyloxyesters later used under optimized conditions are listed in Table 2.

2. Results and discussion

Diastereomerically pure *syn*- or *anti*-α-substituted β-hydroxyesters **1** - **6** were obtained by chemical reduction with Lewis acids in combination with complex borohydrides from the corresponding α-substituted β-ketoesters as previously reported [20] (Table 1). To obtain racemic acyloxyester *rac*-**7** - **12**, required for preparative enzymatic acylation and alcoholysis attempts as well as for comprehensive HPLC studies on their separation, the afore-prepared hydroxyesters **1** - **6** were treated with the appropriate acyl chloride in dry dichloromethane in the presence of pyridine. Under these esterification conditions, acyloxyesters *rac*-**7** - **12** could be synthesized in high yields (77-95%).

2.1. Lipase catalyzed acylation of α-substituted β-hydroxyesters

In a recent lipase screening using compound **1** as substrate (data not shown), we have identified four potent lipases for kinetic resolution. These are Novozyme 435 (N435, immobilized lipase from *Candida antarctica* B = CAL B), immobilized lipase from *Pseudomonas cepacia* (iPCL), lipase from *Pseudomonas* sp. Typ B (PSL B) and lipase from *Candida rugosa* (CRL). Thus, we decided to study these lipases more in detail (particularly with respect to overall conversion and enantioselectivity) using our compounds *rac*-**1** - **6** as target substrates. First, vinyl acetate in *n*-hexane was used as irreversible acyl donor. The reaction was performed in an overhead shaker at 40°C. Conversion was determined using GC-FID and enantioselectivity of the acetylation reaction was analyzed by HPLC on chiral columns. Figs. 2 and 3 summarize the results of the screening.

N435 and PSL B accomplished good performance for compounds *rac*-**1** - **5** over 72 h. In some cases, conversion reached more than 50% indicating unselective acylation over time; noteworthy, 72% of compound *rac*-**3** was converted by PSL B. For hydroxyester *rac*-**6**, moderate conversion was only observed with N435 (max. 29%); the other lipases failed. The performance of CRL and iPCL was generally insufficient. Fig. 3 shows the enantiomeric access (*ee* values) in relation to the conversions of Fig. 1. For all compounds, the highest *ee* values were obtained with N435, followed by PLS B. In the case of hydroxyester *rac*-**1**, an excellent *ee* of ≥99% was achieved with N435 at 59% conversion. Owing to these results, we decided to use N435 in all further experiments. This enzyme preparation has also the advantage of being recoverable due to lipase immobilization on an acrylic resin and it is stable over several reaction cycles [21].

All tested lipases showed preference for the (*3R*)-enantiomer (as we will discuss below). To increase reaction rate and enantioselectivity, we decided to optimize the reaction conditions, particularly for compounds *rac*-**5** and **6**. At first, we studied the influence of the solvent system. In

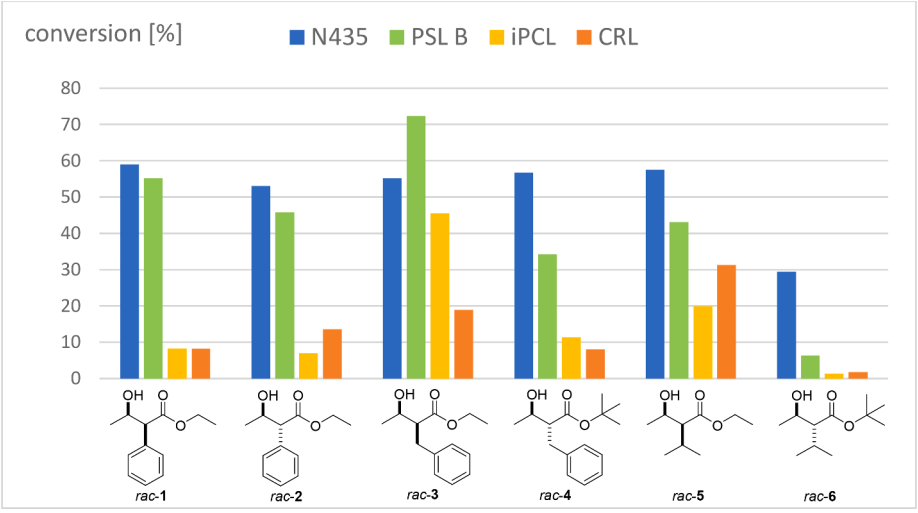

Fig. 2. Conversion of α-substituted β-hydroxyesters by different lipases after 72 h. Reactions were performed in duplicate.

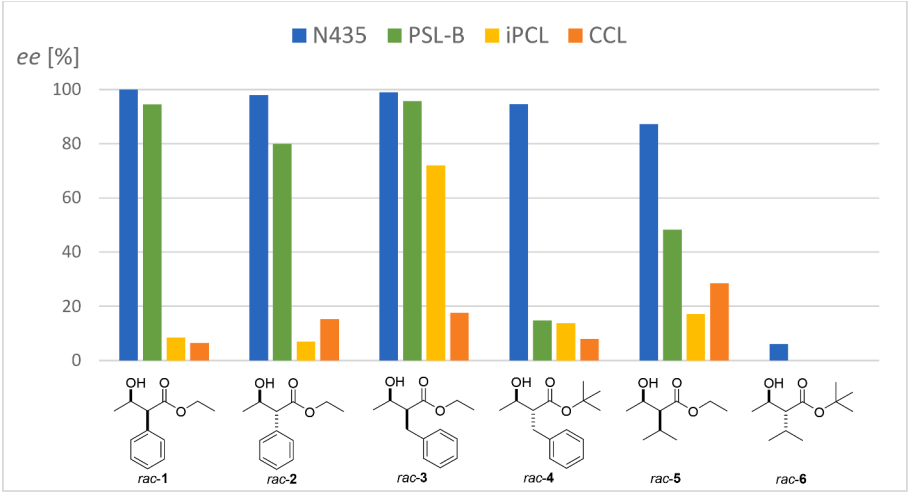

Fig. 3. Enantiomeric excess (*ee*) of α-substituted β-hydroxyesters obtained with four lipases after 72 h. Reactions were performed in duplicate.

Table 3
Influence of the solvent on acylation of *rac*-**1** with vinyl butanoate and Novozyme 435.

Solvent	log *P* [22]	Conversion[a] after 2 h [%]	Conversion[a] after 24 h [%]	*ee*-Value[b] after 24 h [%]
1.4-dioxane	-1.10	<1	<1	n/a
acetone	-0.23	<1	<1	n/a
THF	0.49	<1	2	n/a
chloroform	2.00	<1	<1	n/a
toluene	2.50	10.4	44.0	91
n-hexane	3.50	32.9	47.7	99
n-nonane	5.10	32.1	48.5	98

a) measured by gas chromatography.
b) of hydroxyester (*2R,3S*)-**1**, measured by chiral HPLC.

Table 4
Influence of the acyl donor concentration on the conversion of *rac*-**1**.

Cosubstrate Concentration [mM]	Conversion after 1 h [%]	Decrease of conversion
63 mM VA (1 eq.)	5.5	92%
VA as solvent	0.4	
63 mM VB (1 eq.)	34.5	92%
VB as solvent	2.7	
63 mM VH (1 eq.)	24.5	84%
VH as solvent	3.8	

general, a log *P* value >2 is recommended for enzymatic reactions, since the enzyme conformation strongly depends on the reaction medium [22]. According to literature, the turnover of lipase CAL B tends to increase with decreasing polarity [23]. Seven nonpolar and polar aprotic solvents were tested using the hydroxyester *rac*-**1** as model substrate (Table 3).

Table 3 summarizes the solvent effects on enzymatic conversion and *ee*. The higher the log *P,* the higher was the reaction rate. Conversions in 1,4-dioxane, acetone, THF and chloroform failed (≤ 2%). In addition to unfavorable log *P*, swelling of the PMMA resin matrix of N435 may have affected the enzyme performance in polar solvents by blocking the matrix pores, which eventually stopped lipase reaction. Another disturbance may come from viscosity of the solvent, which causes an opposing effect to polarity and hence could have affected conversion [24].

After 2 h, conversion turned out to be highest in alkane solvents (*n*-hexane, *n*-nonane); obviously, a high log *P* value had a positive effect on the enzymatic reaction. This finding and the fact that *n*-hexane is the solvent of choice was confirmed by good to very good *ee* values for the remaining alcohol (*2R,3S*)-**1** formed in *n*-hexane (99% *ee*) within 24 h (for comparison, 98% *ee* in *n*-nonane and 91% *ee* in toluene). Moreover, *n*-hexane has the advantage over longer-chain alkanes of being easier to remove from the reaction mixture by evaporation. On the other hand, reactants with low boiling point, such as ethyl-3-hydroxy-2-isopropylbutanoate (**5**), cannot be removed under vacuum. Not least, *n*-hexane was the main component of the HPLC eluent, which facilitated the measurement of reaction controls because matrix effects could be excluded.

Since it was reported that the acyl donor influences the performance of the reaction catalyzed by CAL B as well [25], the acylation of *rac*-1 was performed under already established conditions (i.e. in *n*-hexane at 40°C, concentration of the racemic substrate 63 μM) with three vinyl esters (vinyl acetate, VA; vinyl butanoate, VB and vinyl hexanoate, VH) as donors. Results (Table 4) revealed a significant difference in reactivity depending on the carboxylic acid chain length. The best results were obtained with vinyl butanoate as acylation agent. Then, we tried to use the acyl donor as solvent instead of *n*-hexane. This, however, led to a dramatic decrease in reactivity (up to 92%) for all hydroxyesters **1** - **6**.

Table 5
Influence of the acyl donor concentration on the conversion of *rac*-**4**. Reactions were performed in duplicate.

Acyl Donor	Conversion after 6 h	*ee* value of (*2S,3S*)-4
vinyl acetate	28%	42%
vinyl butanoate	47%	98%
vinyl hexanoate	45%	90%

Table 6
Results of kinetic resolution of racemic α-substituted β-hydroxyesters by N435 (CAL B). Reactions were performed in duplicate.

Hydroxyester	Reaction Time [h]	Conversion[a] [%]	*ee*-Value[b] [%]	Yield[c] [%]	E
***syn*-isomers**			***(2R,3S)*-hydroxyester**		
rac-**1**	24	54	≥ 99	44	83
rac-**3**	9	50	99	41	≥100
rac-**5**	96	53	97	40	57
***anti*-isomers**			***(2S,3S)*-hydroxyester**		
rac-**2**	11	51	≥ 99	44	≥100
rac-**4**	24	55	> 99	45	67
rac-**6**	466	45	83	36	n/a[d]

a) measured by GC-FID.
b) hydroxyesters measured on HPLC with chiral columns.
c) after column chromatography (theoretical maximum of 50%).
d) not chemo selective.

The effect was particularly pronounced when small acid moieties with low log *P* values were present (log *P*: VA = 0.5, VB = 1.6, VH = 2.5). Decrease of conversion was observed at concentrations above 250 mM of the vinyl donor. At lower concentrations, vinyl donors just acted as reactants without affecting the solution matrix.

Further effects of the carboxylic acid chain length were studied with regard to the enantioselectivity of *rac*-**4** (Table 5). Vinyl butanoate gave the best results with respect to conversion and enantioselectivity after 6 h reaction time. For the remaining hydroxyester, (*2S,3S*)-**4**, an *ee* value of 98% was ascertained; the *ee* increased to ≥99 % when the time was extended. The same tendency was observed for the hydroxyesters *rac*-**1** - **3** and **6** (results not shown). The only exception was *rac*-**5** that gave the best enantioselectivity with vinyl acetate. Nevertheless, the reaction rate with vinyl butanoate was the highest for all compounds.

Based on these results, we studied kinetic resolution of *syn*- and *anti*-α-substituted β-hydroxyesters, using the hitherto optimized conditions (40°C, *n*-hexane, N435, 0.15 mg/mg hydroxyester, and VB as an acyl donor). Samples were taken from the reaction mixtures after defined times, diluted with *n*-hexane and analyzed by GC-FID and HPLC (on an appropriate chiral column). The latter was only used for the remaining hydroxyesters. However, HPLC analysis of the corresponding enantiomeric acyloxyesters from lipase-catalyzed kinetic resolution was not successful. Results of the up-scaled kinetic resolution are summarized in Table 6. Excellent results were obtained for five out of six hydroxyesters (*rac*-**1** - **5**), demonstrating the catalytic suitability and broad substrate specificity of immobilized CAL B (N435).

For compound *rac*-**6**, we observed the formation of an interesting side product. After some time (>100 h), acetaldehyde appeared in the reaction solution either as the result of acylation or as hydrolysis product of residual water associated with the enzyme. Acetaldehyde in turn reacted with *rac*-**6** to form a hemiacetal that contained a new secondary alcohol moiety (Fig. 4). The latter again favored acylation of the hemiacetal of *rac*-**6** over that of *rac*-**6** itself. Therefore, the yield was only 36% instead of the expected 50%.

Chiral secondary alcohols with stereocenters directly linked to the hydroxyl functionality were enantioselectively resolved by CAL B with the highest efficiency. The two substituents of such a secondary alcohol

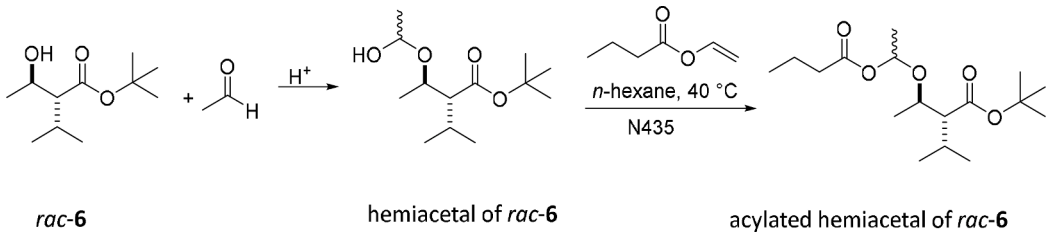

rac-**6** hemiacetal of *rac*-**6** acylated hemiacetal of *rac*-**6**

Fig. 4. Proposed side reaction during the kinetic resolution of *rac*-**6**.

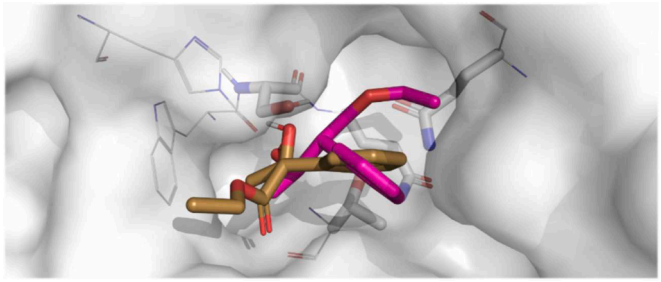

Fig. 5. Docking poses of (*2S,3R*)-**1** (gold) and (*2R,3R*)-**2** (magenta) in the active site of N435. The hydroxyester (*2R,3R*)-**2** is fitted more easily so that the positioning of the substrate is optimal for the acylation to occur.

are referred to as the medium and large sized substituents. In preferred substrates, the medium sized substituent is placed in a small cavity near the catalytic serine (the stereospecificity pocket), while the large substituent will be directed towards the entrance of the enzyme active site. This stereospecificity pocket can only accommodate an ethyl group (or smaller substituent), which explains the low reactivity towards non-preferred configurations with a large substituent longer than the ethyl chain [26].

Conversion of the hydroxyesters *rac*-**1** and *rac*-**2** indicated that the stereocenter in α-position effected the reaction rate of the secondary alcohol moiety. Under the same reaction conditions, *rac*-**1** required twice the reaction time than its diastereomer *rac*-**2** did to achieve a similar result. This could be explained by better fitting of hydroxyester (*2R,3R*)-**2** inside the active center so that the positioning of the substrate is optimal for the acylation to occur. In docking studies, more productive binding poses and shorter distances between substrate methyl group and tryptophane 104 (which lines the stereospecific pocket) were found for hydroxyester (*2R,3R*)-**2** (Fig. 5). The influence of the ester (ethyl or *tert*-butyl) as part of the large substituent was marginal, since these groups protrude from the active site of the enzyme (Fig. 6).

2.2. Lipase catalyzed alcoholysis of α-substituted β-acyloxyesters

Eventually, we obtained substantial amounts of enantiomerically pure (*2R,3S*)-**1, 3, 5** and (*2S,3S*)-**2, 4, 6** α-substituted β-hydroxyesters. The corresponding acyloxyesters enriched during kinetic resolution, (*2S,3R*)-**7, 9, 11** and (*2R,3R*)-**8, 10, 12**, were cleaved by alcoholysis. Since alcohols are not involved in the formation of the intermediate acyl-lipase complex (comprising acylated serine), the deacylation rate is determined by the diffusion of alcohol molecules into the active site of the enzyme [27]. Thus, small aliphatic alcohols diffuse faster into the active site than larger/bulky ones, i.e. the reactivity of the system may decrease with increasing chain length of the alcohol. In addition, nucleophilicity of alcohols decreases with increasing chain length, which can further contribute to decreased reactivity [28]. Accordingly, short-chain alcohols such as ethanol or methanol should ensure highest conversion rates with acylated serine in the active site of lipase [21a].

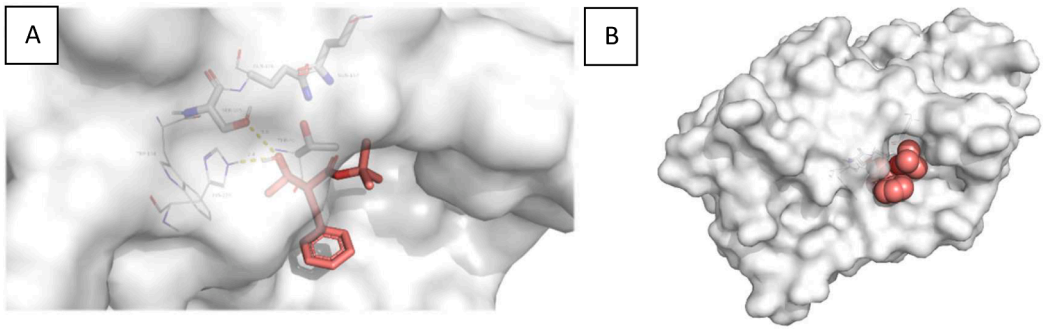

Fig. 6. Docking poses of (*2R,3R*)-**4** in the active site of N435 depicted as sticks (A) and space-filling model (B) model. The ester moieties of *tert*-butylester (*2R,3R*)-**4** is protruding from the active site so that the influence of the reaction rate of ethyl or *tert*-butylester was marginal.

Table 7
Alcoholysis of rac-10 catalyzed by N435 (CAL B) in n-hexane at 40°C. Reactions were performed in duplicate.

Time [h]	Acyloxyester 10 [%]					
	Methanol	Ethanol	1-Butanol	1-Hexanol	1-Octanol	1-Decanol
0	100	100	ß	100	100	100
48	64	70	84	67	62	62
68	63	71	77	59	57	56
91	63	69	69	55	53	53
164	64	71	53	51	51	51
ee [%] (*2R,3R*)-**4** after 164 h	≥ 99	≥ 99	≥ 99	≥ 99	≥ 99	≥ 99

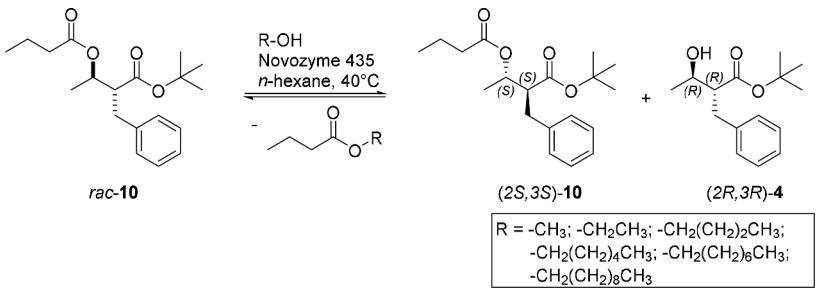

Fig. 7. Alcoholysis of *rac*-**10** to obtain enantiomerically pure (*2R,3R*)-**4**.

Table 8
Results of N435-catalyzed alcoholysis of enantiomerically enriched α-substituted β-acyloxyesters.

Acyloxyester	Reaction time [d]	Conversion[a] [%]	*ee*-Value[b] [%]	Yield[c] [%]
***syn*-isomers**			***(2S,3R)*-hydroxyester**	
(*2S,3R*)-**7**	35	77	≥ 99	65
(*2S,3R*)-**9**	33	85	97	56
***anti*-isomers**			***(2R,3R)*-hydroxyester**	
(*2R,3R*)-**8**	23	82	99	48
(*2R,3R*)-**10**	13	89	≥ 99	70

a) measured by GC-FID.
b) measured hydroxyester on HPLC with chiral columns.
c) after column chromatography (max. 50%).

However, deacylation is more difficult to accomplish than acylation as alcohols can inhibit CAL B (N435). Thus, small alcohols – as polar solvents – tend to detach the essential layer of water molecules (desolvation), which covers and protects the protein. In consequence, lipase conformation is going to change resulting in diminished catalytic activity [29]. Moreover, alcohols can act as unspecific inhibitors of CAL B and may even form dead-end complexes with the lipase protein [30].

N435 catalyzed hydrolysis of acyloxyesters was studied using the alcohols (1 eq.) listed in Table 7 as reactants at 40°C in *n*-hexane; *rac*-**10** was used as model substrate (Fig. 7). Samples were taken from the reaction mixtures over time and analyzed by GC-FID. After 164 h, reactions were stopped by separating the immobilized lipase via filtration. Afterwards, the ratio of enantiomeric hydroxyesters was analyzed by chiral HPLC.

Results of alcoholysis tests are summarized in Table 7. With ethanol and methanol, a rapid incipient reaction was observed, which slowed down to constant product levels of 64% and 70%, respectively, after 48 h. In the case of longer-chain alcohols (1-hexanol, 1-octanol, 1-decanol), the reaction equilibrium was more on the side of products with turnovers around 50% after 164 h. 1-Butanol turned out to be the worst nucleophile for N435-catalyzed alcoholysis. Notably, all obtained hydroxyesters of type (*2R,3R*)-**4** were enantiomerically pure (*ee* ≥ 99%).

The procedure was successfully transferred to acyloxyesters *rac*-**7** and **9**, for which similar reaction rates were observed. In consequence, we decided to use 1-decanol as nucleophilic alcohol for deacylation of the enantiomerically enriched acyloxyesters (*2S,3R*)-**7, 9** and (*2R,3R*)-**8, 10**. Maximum reaction rate was determined at an enzyme load of 500 mg N435/ 0.1 mmol substrate, which is two orders higher than that for the acylation reaction (3 mg/ 0.1 mmol substrate). Results of respective alcoholyses are given in Table 8.

They indicate high conversion along with excellent *ee* values between 97 and ≥99%. However, substantial shortcomings of these enzymatic deacylations are the long reaction time ranging from several days to weeks as well as the demand for large amounts of immobilized CAL B (N435). This gave rise to unwanted side reactions such as transesterification of ethyl esters.

(*2R,3R*)-**10** showed the highest alcoholysis rate (79% conversion within 6 days), despite of its sterically demanding *tert*-butyl group in the acyloxyester molecule. Interestingly, transesterification was not observed in this case, which may be due to steric hindrance of the nucleophiles. Furthermore, we observed that the configuration in α-position, besides that of carbinol, affected the reactivity as well. Thus, enriched (*2R,3R*)-**10** showed higher reactivity compared to the diastereomer (*2S,3R*)-**7**. This tendency was already ascertained in the acylation of the pair *rac*-**1** and *rac*-**2** (Table 6).

The isopropyl substituted enantiomers (*2S,3R*)-**10** and (*2R,3R*)-**11** enriched by kinetic resolution did not show any conversion under the reaction conditions described above. Probably, the substrate was sterically too demanding and did hardly diffuse into the active side of N435 (CAL B). The reaction times of preceding acylation of **5** and **6** support this assumption. Hence, acyloxyesters (*2S,3R*)-**10** and (*2R,3R*)-**11** were chemically saponified with aqueous potassium hydroxide.

2.3. Determination of the absolute configuration by NMR-spectroscopy

Finally, the absolute configurations of separated enantiomer pairs of each α-substituted β-hydroxyester were determined by Mosher's method [31]. To this end, (*R*)-Mosher's acid chloride [(*R*)-MTPA-Cl] was used to derivatize the enantiomerically pure hydroxyesters (*2R,3S*)-**1, 3, 5** and (*2S,3S*)-**2, 4, 6**. As reference, racemic hydroxyesters **1** - **6** were also esterified with (*R*)-MTPA-Cl. After derivatization and purification by liquid column chromatography, all (*S*)-MTPA-esters were analyzed by ^{1}H-NMR spectroscopy to determine the characteristic chemical shift of each enantiomer. The derivatizing reactions were performed in dry dichloromethane supplemented with (*R*)-MTPA-Cl, the respective hydroxyester and pyridine to obtain the corresponding MTPA-esters **13-24** in quantitative yields (Fig. 8).

The phenyl-ring is known to impose an anisotropic, magnetic shielding effect on protons residing above (or below) the plane of the aryl ring. This shielding results in a more up-field chemical shift for the affected protons in the ^{1}H-NMR spectrum. Fig. 9 shows the mostly

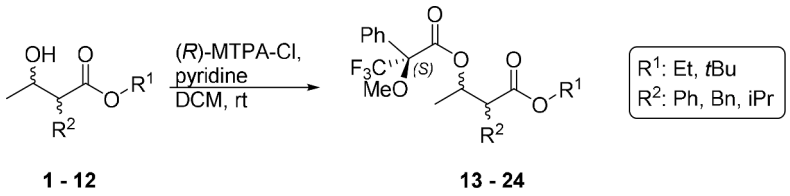

Fig. 8. Derivatization of α-substituted β-hydroxyesters with (*R*)-MTPA-Cl.

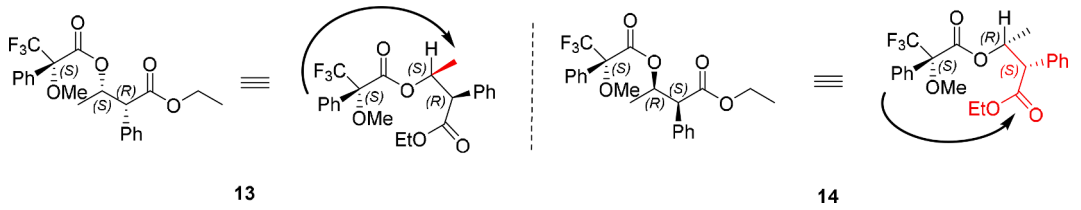

Fig. 9. Most populated conformer of the (*R*)-MTPA ester of *rac*-**1**. Arrows in respective formula representations (red moieties) mark shielding effects of the phenyl group.

populated rotamer where the methyl group of (*2R,3S*)-**1** is *syn*-periplanar to the phenyl ring of (*R*)-MPTA, resulting in a high-field shift. Thus, the methyl group of (*2S,3R*)-**1** was found at lower field, while the rest of the molecule shifted to higher field. These shielding effects decreased with increasing distance to the aryl ring of MTPA.

To quantify the difference in chemical shift, following equations were used for *syn*-hydroxyesters and *anti*-isomers, respectively: $\Delta\delta_{(2S,3R)/(2R,3S)} = \delta_{(2S,3R)} - \delta_{(2R,3S)}$ and $\Delta\delta_{(2R,3R)/(2S,3S)} = \delta_{(2R,3R)} - \delta_{(2S,3S)}$. The methyl group in γ-position was used for calculation, since it is not superimposed with other signals and just appears as a duplet. All examined MTPA-esters from hydroxyesters **1** - **7** showed a positive difference in chemical shift in the range from 0.05 to 0.10 ppm of the γ-methyl group for enantiomers in (*3S*)-configuration. These findings strongly indicate that N435 (CAL B) exhibits (*3R*)-stereo-preference towards racemic α-substituted β-hydroxyesters, which is in accordance with the steric binding model of Kazlauskas et al.[32]

3. Conclusions

We describe a reliable lipase-catalyzed approach for the preparation of enantiomerically pure α-substituted β-hydroxyesters to be used as potential chiral building blocks. Four free or immobilized lipases were tested for enantioselective acylation with respect to conversion and enantioselectivity. Our method includes a two-step kinetic resolution using immobilized lipase B from *Candida antarctica* (CAL B, Novozyme 435 = N435) as most appropriate biocatalyst that could be recovered after reaction (even if the re-use of the enzyme was not quantitatively investigated). The influence of enzymatic reaction parameters, such as solvent type, acyl donor and its concentration as well as alcohol chain length, on the stereochemical performance of kinetic resolution was studied and optimized. Under the latter conditions, we obtained high yields of both enantiomers of all α-substituted β-hydroxyesters (up to ≥99%). Beyond that, we demonstrated the limits of lipase-catalyzed resolution for demanding substrates such as the α-isopropyl β-hydroxyesters; in this case, the reaction time of acylation was unsatisfactory and alcoholysis did not occur. We determined the absolute configuration of all enantiomerically pure β-hydroxyesters according to the method of Mosher, which proved the (*3R*)-stereo-preference of Novozyme 435 (N435) towards racemic α-substituted β-hydroxyesters.

4. Experimental

4.1. Analytical and general procedures

^{1}H-NMR spectra were recorded at 400 MHz and for ^{13}C at 101 MHz with a Bruker Ascend NMR-spectrometer. As reference peak, TMS or the deuterated solvent was used. All reactions were performed in oven-dried glassware under a positive pressure of nitrogen and stirring with a magnet. Liquid column chromatography was carried out on silica gel (40-63 μm mesh) using a solvent mixture of ethyl acetate and *n*-hexane as eluent. Thin layer chromatography (TLC) was performed using 0.25-mm E. Merck precoated silica gel plates (60F-254). Diastereomeric purity was determined by gas chromatography (GC) on an Agilent 7890A system with flame ionization detector (FID). The GC device was equipped with a VF-5ms column (30 m × 0.25 mm × 0.25 μm, Agilent) and GC parameters were chosen as follows: inlet - 250°C, flow - 1.2 mL/min (N_2), oven -70°C to 270°C (10°C/min), detector temperature - 300°C. Enantiomeric excesses (% *ee*) of the hydroxyesters were determined by HPLC on a Thermo Fisher Scientific Ultimate 3000 system, equipped with a UV detector and chiral Phenomenex columns (Lux 5 μm i-Amylose-1, LC Column 250 mm x 4.6 mm; Lux 5 μm Cellulose-3, LC Column 250 mm x 4.6 mm) eluted with mixtures of *n*-hexane/ isopropanol as the mobile phase in the appropriate ratios given in the supporting information. MM2 force field was calculated with the Software "*Chem3D*" (version 17.0).

4.2. Chemical material

Commercial grade reagents and solvents were used without further purification. Solvents were dried and purified as recommended [33]. Lipases including immobilized CAL B (Novozymes 435 = N435) were purchased from Sigma Aldrich. Specific features of Novozymes lipases are reported in the brochure "Immobilized lipases for biocatalysis" [21a]. Enzymatic reactions were discontinuously performed in an overhead shaker (15 min^{-1}).

4.3. Computational

To analyze favorable ligand binding geometries for the substrates AutoDock Vina 1.1.2 were carried out [34]. Ligand molecules were prepared with ChemDraw (version 17.0 and saved in PDB format. Gasteiger partial charges were calculated with AutoDockTools 1.5.6rc3 [35], and the final ligand files were prepared in PDBQT format.

The crystallographic structure of lipase from *Candida antarctica* B (CAL B, PDB code 5A71) was downloaded from RCSB Protein Data Bank (PDB, http://www.rcsb.org/pdb/). Chain A of the crystallographic structure was chosen (open conformation of CAL B [36] and rotated to adjust fitting in searching grid box of AutoDockTools using PyMOL [37] The pdb file was prepared by AutoDockTools, all nonstandard (nonprotein) molecules including the two sugar units (NAG) and crystal waters were removed, the polar hydrogen atoms were added, and Gasteiger charges were calculated. With use of AutoDockTools, a searching grid box was set in the appropriate size before docking. The box center was set at catalytic Ser105 of CAL B. Docking was performed in a 40 × 50 × 40 unit grid box centered on the enzyme active site (center_x = -39.285, center_y = 29.55, center_z = -23.294) with a grid spacing of 0.325 Å. Docking was performed with an exhaustiveness level of 100. The docking results of each ligand were ranked based on free binding energy (kcal/mol). The best twenty poses (modes) within an energy range of 3 kcal/mol were selected according to AutoDock Vina scoring functions mainly based on binding energies and show mutual affinity (kcal/mol). Each selected binding mode was manually inspected in order to select only productive conformations where the substrate assumes a Near Attack Conformation (NAC) compatible with the attack of the catalytic serine (Ser105) to the carbon atom of the acyl group of the ligand. Each docking was repeated ten times for each substrate. The analyses of interactions of docked ligand conformations in the CAL B active site were performed and visualized with PyMOL.

4.4. Diastereoselective syntheses of α-substituted β-hydroxyesters rac-1 - 6

Diastereoselective reduction starting from the corresponding α-substituted β-ketoesters was reported recently [20].

4.5. General procedure for chemical acylation of α-substituted β-hydroxyesters rac-1 - 6

In a dry 50-mL reaction vessel, the respective hydroxyester (1 eq.) was dissolved in absolute DCM (2.5 mL/mmol hydroxyester) and mixed with pyridine (3 eq.). Acid chloride (2 eq.) was added at 0°C. The mixture was stirred overnight at room temperature and then acidified with HCl 1N to pH 3. Afterwards, the same amount of water was added. The phases were separated and the aqueous layer was extracted two more times with DCM. The organic phases were dried over Na_2SO_4, filtered and concentrated under vacuum. The crude product was purified by column chromatography (*n*-hexane: ethyl acetate = 95:5) using silica gel to obtain the α-substituted β-hydroxyesters *rac*-**7** - **12**.

***syn*-Ethyl-3-(butyryloxy)-2-phenylbutanoate (7)**

Yield: 129 mg (95%)

^{1}H-NMR (400 MHz, $CDCl_3$) δ in ppm: 7.36 - 7.24 (m, 5H, aromat.), 5.56 (dq, ^3J = 9.0 Hz, ^3J = 6.2 Hz 1H, β-C*H*), 4.21 - 4.07 (m, 2H, O-CH_2-CH_3), 3.71 (d, ^3J = 9.0 Hz, 1H, α-C*H*), 2.11 - 1.97 (m, 2H, CH_2-CH_2-CH_3), 1.43 - 1.30 (m, 2H, CH_2-CH_2-CH_3), 1.31 (d, ^3J = 6.2 Hz, 3H, HOCH-CH_3), 1.22 (t, ^3J = 7.1 Hz, 3H, O-CH_2-CH_3), 0.72 (t, ^3J = 7.4 Hz, 3H, CH_2-CH_2-CH_3)

^{13}C-NMR (101 MHz, $CDCl_3$) δ in ppm: 172.57 (C=O), 171.28 (C=O), 135.51 (C-1 aromat.), 128.78 (C-3 aromat.), 128.39 (C-2 aromat.), 127.61 (C-4 aromat.), 70.49 (β-*C*), 61.03 (O-*C*H_2-CH_3), 57.37 (α-*C*), 36.25 (*C*H_2-CH_2-CH_3), 18.79 (CH_2-*C*H_2-CH_3), 18.26 (HOCH-*C*H_3), 14.06 (O-CH_2-*C*H_3), 13.39 (CH_2-CH_2-*C*H_3)

***anti*-Ethyl-3-(butyryloxy)-2-phenylbutanoate (8)**

Yield: 129 mg (95%)

^{1}H-NMR (400 MHz, $CDCl_3$) δ in ppm: 7.37 - 7.27 (m, 5H, aromat.), 5.50 (dq, ^3J = 10.5 Hz, ^3J = 6.2 Hz 1H, β-C*H*), 4.19 - 4.04 (m, 2H, O-CH_2-CH_3), 3.68 (d, ^3J = 10.5 Hz, 1H, α-C*H*), 2.26 (t, ^3J = 7.4 Hz, 2H, CH_2-CH_2-CH_3), 1.65 (sext, ^3J = 7.3 Hz, 2H, CH_2-CH_2-CH_3), 1.21 (t, ^3J = 7.1 Hz, 3H, O-CH_2-CH_3), 1.04 (d, ^3J = 6.2 Hz, 3H, HOCH-CH_3), 0.95 (t, ^3J = 7.4 Hz, 3H, CH_2-CH_2-CH_3)

^{13}C-NMR (101 MHz, $CDCl_3$) δ in ppm: 172.61 (C=O), 171.51 (C=O), 135.00 (C-1 aromat.), 128.85 (C-3 aromat.), 128.63 (C-2 aromat.), 128.02 (C-4 aromat.), 71.72 (β-*C*), 60.91 (O-*C*H_2-CH_3), 57.84 (α-*C*), 36.45 (*C*H_2-CH_2-CH_3), 18.45 (CH_2-*C*H_2-CH_3), 17.79 (HOCH-*C*H_3), 14.11 (O-CH_2-*C*H_3), 13.63 (CH_2-CH_2-*C*H_3)

***syn*-Ethyl-2-benzyl-3-(butyryloxy)butanoate (9)**

Yield: 514 mg (88%)

^{1}H-NMR (400 MHz, $CDCl_3$) δ in ppm: 7.28 - 7.26 (m, 2H, aromat.), 7.21 - 7.14 (m, 3H, aromat.), 5.19 - 5.13 (m, 1H, β-C*H*), 4.08 - 3.97 (m, 2H, O-CH_2-CH_3), 2.96 - 2.84 (m, 3H, α-C*H*, Ph-CH_2), 2.28 (t, ^3J = 7.4 Hz, 2H, CH_2-CH_2-CH_3), 1.66 (sext, ^3J = 7.3 Hz, 2H, CH_2-CH_2-CH_3), 1.29 (d, ^3J = 6.4 Hz, 3H, HOCH-CH_3), 1.10 (t, ^3J = 7.1 Hz, 2H, O-CH_2-CH_3), 0.96 (t, ^3J = 7.4 Hz, 2H, CH_2-CH_2-CH_3)

^{13}C-NMR (101 MHz, $CDCl_3$) δ in ppm: 172.87 (C=O), 172.35 (C=O), 138.66 (C-1 aromat.), 128.77 (C-3 aromat.), 128.40 (C-2 aromat.), 126.43 (C-4 aromat.), 70.51 (β-*C*), 60.49 (O-*C*H_2-CH_3), 57.37 (α-*C*), 36.41 (*C*H_2-CH_2-CH_3), 34.71 (Ph-*C*H_2), 18.45 (CH_2-*C*H_2-CH_3), 17.72 (HOCH-*C*H_3), 14.07 (O-CH_2-*C*H_3), 13.67 (CH_2-CH_2-*C*H_3)

***anti-tert*-Butyl-2-benzyl-3-(butyryloxy)butanoate (10)**

Yield: 304 mg (95%)

^{1}H-NMR (400 MHz, $CDCl_3$) δ in ppm: 7.28 - 7.24 (m, 2H, aromat.), 7.21 - 7.15 (m, 3H, aromat.), 5.13 (p, 1H, ^3J = 6.4 Hz, 2H, β-C*H*), 2.99 - 2.77 (m, 3H, α-C*H*, Ph-CH_2), 2.31 - 2.19 (m, 2H, CH_2-CH_2-CH_3), 1.65 (sext, ^3J = 7.4 Hz, 2H, CH_2-CH_2-CH_3), 1.31 (d, ^3J = 6.4 Hz, 3H, HOCH-CH_3), 1.29 (s, 9H, C(CH_3)$_3$), 0.93 (t, ^3J = 7.4 Hz, 3H, CH_2-CH_2-CH_3)

^{13}C-NMR (101 MHz, $CDCl_3$) δ in ppm: 172.68 (C=O), 171.37 (C=O), 138.71 (C-1 aromat.), 129.01 (C-3 aromat.), 128.30 (C-2 aromat.), 126.36 (C-4 aromat.), 80.68 (*C*(CH$_3$)$_3$), 70.85 (β-*C*), 53.50 (α-*C*), 36.37 (*C*H_2-CH_2-CH_3), 34.34 (Ph-*C*H_2), 27.87 (C(*C*H$_3$)$_3$), 18.42 (CH_2-*C*H_2-CH_3), 17.80 (HOCH-*C*H_3), 13.69 (CH_2-CH_2-*C*H_3)

***syn*-Ethyl-3-acetoxy-2-isopropylbutanoate (11)**

Yield: 474 mg (88%)

^{1}H-NMR (400 MHz, $CDCl_3$) δ in ppm: 5.18 (dq, ^3J = 7.6 Hz, ^3J = 6.4 Hz 1H, β-C*H*), 4.22 - 4.11 (m, 2H, O-CH_2-CH_3), 2.49 (d, ^3J = 7.8 Hz, 1H, α-C*H*), 2.03 (s, 1H, CO-CH_3), 2.03 - 1.94 (m, 1H, C*H*(CH$_3$)$_2$), 1.27 (t, ^3J = 7.1 Hz, 3H, O-CH_2-CH_3), 1.27 (d, 3H, d, ^3J = 6.2 Hz, 3H, HOCH-CH_3), 0.98 (d, ^3J = 6.8 Hz, 3H, CH(CH_3)$_2$), 0.91 (d, ^3J = 6.7 Hz, 3H, CH(CH_3)$_2$)

^{13}C-NMR (101 MHz, $CDCl_3$) δ in ppm: 172.43 (C=O), 170.23 (C=O), 69.50 (β-*C*), 60.15 (O-*C*H_2-CH_3), 56.28 (α-*C*), 21.24 (CO-*C*H_3), 21.24 (CH(*C*H$_3$)$_2$), 20.51 (CH(*C*H$_3$)$_2$), 16.64 (HOCH-*C*H_3), 14.39 (O-CH_2-*C*H_3)

***anti-tert*-Butyl-3-(butyryloxy)-2-isopropylbutanoate (12)**

Yield: 205 mg (77 %)

^{1}H-NMR (400 MHz, $CDCl_3$) δ in ppm: 5.18 (dq, ^3J = 7.9 Hz, ^3J = 6.3 Hz 1H, β-C*H*), 2.29 – 2.19 (m, 3H, α-C*H*, CH_2-CH_2-CH_3), 1.95 (oct, ^3J = 6.8 Hz, 1H, C*H*(CH$_3$)$_2$), 1.64 (sext, ^3J = 7.4 Hz, 2H, CH_2-CH_2-CH_3), 1.45 (s, 9H, C(CH_3)$_3$), 1.24 (d, ^3J = 6.3 Hz, 3H, HOCH-CH_3), 0.99 (d, ^3J = 6.9 Hz, 3H, CH(CH_3)$_2$), 0.94 (d, ^3J = 7.2 Hz, 3H, CH(CH_3)$_2$), 0.9 (t, ^3J = 7.2 Hz, 3H, CH_2-CH_2-CH_3)

^{13}C-NMR (101 MHz, $CDCl_3$) δ in ppm: 172.80 (C=O), 171.44 (C=O), 80.45 (*C*(CH$_3$)$_3$), 69.53 (β-*C*), 57.98 (α-*C*), 36.46 (*C*H_2-CH_2-CH_3), 28.14 (C(*C*H$_3$)$_3$), 27.07 (CH(*C*H$_3$)$_2$), 21.21 (CH(*C*H$_3$)$_2$), 18.59 (CH(*C*H$_3$)$_2$), 18.45 (CH_2-*C*H_2-CH_3), 18.11 (HOCH-*C*H_3), 13.68 (CH_2-CH_2-*C*H_3)

4.6. General procedure for lipase screening of rac-1 - 6

The respective lipase (6 mg) was weighed into a 1.5-mL vial and suspended in *n*-hexane (1.2 mL). The hydroxyester (0.6 μmol) and vinyl acetate (0.54 mmol, 50 μL) were added and allowed to react for 72 h in an overhead shaker at 40°C. After 72 h, reaction was stopped by filtering the solution (45-μm pore size) to remove the enzyme. Enzymatic conversion was followed by gas chromatography and the enantiomeric ratios were determined by HPLC on chiral columns.

4.7. General procedure for enantioselective acylation of rac-1 - 6 with Novozyme 435

Hydroxyesters **1** - **6** (1 eq.) were weighed into a sealed reaction vessel, the vinyl donor (1.3 eq.) was added and the solution diluted with *n*-hexane (1 mL/ 33 mg hydroxyester). Immobilized CAL B (0.15 mg/mg hydroxyester) was supplemented and the suspension allowed reacting discontinuously in an overhead shaker at 40°C. Reaction control was performed by gas chromatography. Enantioselectivity was proven by chiral HPLC. After completing the reaction, the immobilized enzyme was separated by filtration and washed several times with *n*-hexane. Afterwards, the reaction solution was concentrated under vacuum and the acylated product purified by column chromatography (*n*-hexane: ethyl acetate = 9:1 to 8:2) on silica gel.

(*2R,3S*)-Ethyl-3-hydroxy-2-phenylbutanoate ((*2R,3S*)-1)

Vinyl butanoate was used as vinyl donor. After 24 h of reaction, (*2R,3S*)-**1** was obtained as colorless oil.

Yield: 222 mg (44%); *ee* ≥ 99%

(*2S,3S*)-Ethyl-3-hydroxy-2-phenylbutanoate ((*2S,3S*)-2)

Vinyl butanoate was used as vinyl donor. After 10 h of reaction, (*2S,3S*)-**2** was obtained as colorless oil.

Yield: 87 mg (44%); *ee* ≥ 99%

(*2R,3S*)-Ethyl-2-benzyl-3-hydroxybutanoate ((*2R,3S*)-3)

Vinyl butanoate was used as vinyl donor. After 9 h of reaction, (*2R,3S*)-**3** was obtained as colorless oil.

Yield: 207 mg (41%); *ee* = 99%

(*2S,3S*)-*tert*-Butyl-2-benzyl-3-hydroxybutanoate ((*2S,3S*)-4)

Vinyl butanoate was used as vinyl donor. After 24 h of reaction, (*2S,3S*)-**4** was obtained as colorless solid.

Yield: 227 mg (45%); *ee* ≥ 99%

(*2R,3S*)-Ethyl-3-hydroxy-2-isopropylbutanoate ((*2R,3S*)-5)

Vinyl acetate was used as vinyl donor. After 96 h of reaction, (*2R,3S*)-**5** was obtained as colorless oil.

Yield: 201 mg (40%); *ee* = 97%

(*2S,3S*)-*tert*-Butyl-3-hydroxy-2-isopropylbutanoate ((*2S,3S*)-6)

Vinyl acetate was used as vinyl donor. After 466 h of reaction, (*2S,3S*)-**6** was obtained as colorless oil.

Yield: 179 mg (36%); *ee* = 83%

4.8. General procedure for enantioselective alcoholysis of 7 - 10 with Novozyme 435 (N435)

Acyloxyester **7** - **10** (1 eq.) was weighed into a sealed reaction vessel and 1-decanol (1.1 eq.) was added. The solution was diluted with *n*-hexane (15 mL/ mmol acyloxyester). Immobilized CAL B (N435, 5 g/ mmol acyloxyester) was added to the mixture and the suspension was allowed to react in an overhead shaker at 40°C discontinuously. Reaction progress was controlled by gas chromatography. After stagnation of the conversion, additional 1-decanol (0.2 eq.) was added. When no more conversion was observed, the mixture was filtered and the immobilized enzyme washed several times with *n*-hexane (for re-use). The filtrate was concentrated under vacuum and the hydroxyester purified by column chromatography (*n*-hexane: ethyl acetate = 9:1 to 8:2) using silica gel.

(*2S,3R*)-Ethyl-3-hydroxy-2-phenylbutanoate ((*2S,3R*)-1)

After 35 days of reaction (*2S,3R*)-**1** was obtained as colorless oil.

Yield: 156 mg (65%); *ee* ≥ 99%

(*2R,3R*)-Ethyl-3-hydroxy-2-phenylbutanoate ((*2R,3R*)-2)

After 23 days of reaction (*2R,3R*)-**2** was obtained as colorless oil.

Yield: 18 mg (48%); *ee* = 99%

(*2S,3R*)-Ethyl-2-benzyl-3-hydroxybutanoate ((*2S,3R*)-3)

After 33 days of reaction (*2S,3R*)-**3** was obtained as colorless oil.

Yield: 117 mg (56%); *ee* = 97%

(*2R,3R*)-*tert*-Butyl-2-benzyl-3-hydroxybutanoate ((*2R,3R*)-4)

After 13 days of reaction (*2R,3R*)-**4** was obtained as colorless solid.

Yield: 143 mg (70%); *ee* ≥ 99%

(*2S,3R*)-Ethyl-3-hydroxy-2-isopropylbutanoate ((*2S,3R*)-5)

In a round bottom flask, acyloxyester (*2S,3R*)-**11** (268 mg; 1.24 mmol) was dissolved in ethanol (10 mL) and aqueous KOH (1 N; 4.96 mmol; 4.96 mL; 4 eq.) was added at room temperature. The mixture was stirred until no more starting material was observed (reaction control by GC). After completion of the reaction (after about 3 h), ethanol was removed under vacuum. The residue was extracted with diethyl ether (3 × 20 mL) and the collected organic phases were washed with brine. The etheric phase was dried over Na_2SO_4, filtered and concentrated under vacuum. The crude product was purified by column chromatography (*n*-hexane: ethyl acetate = 8:2) on silica gel to obtain (*2S,3R*)-**5** as colorless oil.

Yield: 155 mg (72%); *ee* = 70%

(*2R,3R*)-*tert*-butyl-3-hydroxy-2-isopropylbutanoate ((*2R,3R*)-6)

In a round bottom flask, acyloxyester (*2S,3S*)-**12** (284 mg; 1.04 mmol) was dissolved in ethanol (15 mL) and aqueous KOH (1 N; 5.21 mmol; 5.21 mL; 5 eq.) was added at room temperature. The mixture was stirred at 50°C until no more starting material was observed (reaction control by GC). After completion of the reaction (after 3 h), ethanol was removed under vacuum. The residue was extracted with diethyl ether (3 × 20 mL) and the collected organic phases were washed with brine. The etheric phase was dried over Na_2SO_4, filtered and concentrated under vacuum. The crude product was purified by column chromatography (*n*-hexane: ethyl acetate = 8:2) on silica gel to obtain (*2R,3R*)-**6** as colorless oil.

Yield: 155 mg (72%); *ee* = 98%

4.9. General procedure for acylation reactions with (R)-MTPA-Cl

In a 1.5-mL vial, the respective hydroxyester (66 μmol, 1 eq.) was dissolved in absolute DCM (1 mL) and mixed with dry pyridine (22 μL, 270 μmol, 3 eq.) under nitrogen. (*R*)-MTPA-Cl (32 μL, 171 μmol, 2 eq.) was added under stirring at room temperature. The obtained mixture was further stirred for two h (ethyl ester) or overnight (*tert*-butylester). After the reaction had been completed, the mixture was partitioned between diethyl ether (3 mL) and water (1 mL). The two phases were separated in a separatory funnel. The aqueous phase was extracted with diethyl ether (3 mL) and the combined organic phases were washed again with a small amount of water. The organic phase was dried over Na_2SO_4, filtered and the solvent removed under vacuum. The crude (*S*)-MTPA ester was further purified by column chromatography (*n*-hexane: ethyl acetate = 9:1) on silica gel. The MTPA esters were obtained as colorless oils in quantitative yields.

(*2R,3S*)-**1**-(*S*)-MTPA (**13**):

^{1}H-NMR (400 MHz, DMSO-d_6) δ in ppm: 7.46 – 7.39 (m, 1H), 7.39 – 7.27 (m, 7H), 7.14 (d, ^3J = 7.6 Hz, 2H), 5.73 (dq, ^3J = 8.4 Hz, ^3J = 6.1 Hz, 1H), 4.16 – 4.04 (m, 2H), 4.02 (d, ^3J = 8.4 Hz, 1H), 3.12 (d, ^3J = 1.2 Hz, 3H), 1.25 (d, ^3J = 6.2 Hz, 3H), 1.12 (t, ^3J = 7.1 Hz, 3H)

^{13}C-NMR (101 MHz, DMSO-d_6) δ in ppm: 170.67, 165.03, 134.95, 131.59, 129.74, 128.90, 128.62, 128.50, 127.91, 126.76, 123.41 (q, $^1J_{C\text{-}F}$ = 290 Hz), 84.13 (q, $^2J_{C\text{-}F}$ = 24 Hz), 73.48, 60.96, 55.37, 54.81, 17.90, 13.85

(*2S,3R*)-**1**-(*S*)-MTPA (**14**):

^{1}H-NMR (400 MHz, DMSO-d_6) δ 7.47 – 7.33 (m, 4H), 7.30 – 7.14 (m, 7H), 5.81 – 5.73 (m, 1H), 4.08 – 4.00 (m, 3H), 3.24 (s, 3H), 1.30 (d, ^3J = 6.3 Hz, 3H), 1.10 (t, ^3J = 7.1 Hz, 3H)

^{13}C-NMR (101 MHz, DMSO-d_6) δ in ppm: 170.53, 164.84, 134.48, 131.27, 129.62, 129.04, 128.44, 128.27, 127.66, 126.87, 123.51 (q, $^1J_{C\text{-}F}$ = 290 Hz), 84.06 (q, $^2J_{C\text{-}F}$ = 24 Hz), 73.07, 60.80, 55.14, 54.97, 18.03, 13.81

(*2S,3S*)-**2**-(*S*)-MTPA (**15**):

^{1}H-NMR (400 MHz, DMSO-d_6) δ in ppm: 7.53 – 7.43 (m, 5H), 7.42 – 7.28 (m, 5H), 5.63 (dq, ^3J = 10.6 Hz, 6.2 Hz, 1H), 4.14 – 3.95 (m, 3H), 3.47 (s, 3H), 1.08 (t, ^3J = 7.1 Hz, 3H), 1.00 (d, ^3J = 6.3 Hz, 3H)

^{13}C-NMR (101 MHz, DMSO-d_6) δ in ppm: 171.26, 165.03, 134.37, 131.58, 129.95, 129.06, 128.59, 128.35, 128.25, 127.01, 123.05 (q, $^1J_{C\text{-}F}$ = 290 Hz), 84.13 (q, $^2J_{C\text{-}F}$ = 27 Hz) 74.41, 60.87, 55.35, 55.18, 16.59, 13.77

(*2R,3R*)-**2**-(*S*)-MTPA (**16**):

^{1}H-NMR (400 MHz, DMSO-d_6) δ in ppm: 7.52 – 7.42 (m, 5H), 7.41 – 7.31 (m, 5H), 5.63 (dq, ^3J = 10.7 Hz, ^3J = 6.3 Hz, 1H), 3.95 (d, ^3J = 10.5 Hz, 1H), 3.92 – 3.79 (m, 2H), 3.49 (d, ^3J = 1.1 Hz, 3H), 1.10 (d, ^3J = 6.3 Hz, 3H), 0.98 (t, ^3J = 7.1 Hz, 3H)

^{13}C-NMR (101 MHz, DMSO-d_6) δ in ppm: 171.27, 165.03, 134.38, 131.58, 129.95, 129.06, 128.60, 128.35, 128.25, 127.01, 123.10 (q, $^1J_{C\text{-}F}$ = 290 Hz), 84.14 (q, $^2J_{C\text{-}F}$ = 27 Hz), 74.41, 60.88, 55.35, 55.19, 16.59, 13.78

(*2S,3R*)-**3**-(*S*)-MTPA(**17**):

^{1}H-NMR (400 MHz, DMSO-d_6) δ in ppm: 7.49 (s, 5H), 7.31 – 7.24 (m, 2H), 7.23 – 7.15 (m, 3H), 5.37 (qd, ^3J = 6.3 Hz, ^3J = 5.2 Hz, 1H), 3.94 (q, ^3J = 7.1 Hz, 2H), 3.51 (s, 1H), 3.08 (dt, ^3J = 9.4 Hz, ^3J = 5.4 Hz, 1H), 2.92 – 2.81 (m, 2H), 1.30 (d, ^3J = 6.4 Hz, 3H), 0.98 (t, ^3J = 7.1 Hz, 3H)

^{13}C-NMR (101 MHz, DMSO-d_6) δ in ppm: 171.50, 165.06, 138.40, 131.41, 129.93, 128.71, 128.62, 128.33, 127.16, 126.41, 123.16 (q, $^{1}J_{C-F}$ = 289 Hz), 84.17 (q, $^{2}J_{C-F}$ = 27 Hz), 73.54, 60.26, 55.30, 50.81, 33.05, 16.40, 13.72

(*2R,3S*)-**3**-(*S*)-MTPA (**18**):

^{1}H-NMR (400 MHz, DMSO-d_6) δ in ppm: 7.52 – 7.44 (m, 5H), 7.29 – 7.15 (m, 3H), 7.12 – 7.04 (m, 2H), 5.37 – 5.27 (m, 1H), 3.91 – 3.84 (m, 2H), 3.50 (s, 3H), 2.98 (dt, ^{3}J = 8.4 Hz, ^{3}J = 6.3 Hz, 1H), 2.76 – 2.67 (m, 2H), 1.39 (d, ^{3}J = 6.4 Hz, 3H), 0.96 (t, ^{3}J = 7.1 Hz, 3H)

^{13}C-NMR (101 MHz, DMSO-d_6) δ in ppm: 171.36, 165.05, 138.33, 131.46, 129.94, 128.71, 128.63, 128.33, 127.08, 126.40, 123.16 (q, $^{1}J_{C-F}$ = 289 Hz), 84.17 (q, $^{2}J_{C-F}$ = 27 Hz), 73.54, 60.22, 55.30, 51.11, 33.05, 16.95, 13.72

(*2S,3S*)-**4**-(*S*)-MTPA(**19**):

^{1}H-NMR (400 MHz, DMSO-d_6) δ 7.54 – 7.43 (m, 5H), 7.33 – 7.24 (m, 2H), 7.24 – 7.18 (m, 3H), 5.28 (p, ^{3}J = 6.5 Hz, 1H), 3.49 (s, 2H), 2.98 – 2.84 (m, 2H), 2.73 (dd, ^{2}J = 13.4 Hz, ^{3}J = 10.7 Hz, 1H), 1.34 (d, ^{3}J = 6.3 Hz, 3H), 1.12 (s, 9H)

^{13}C-NMR (101 MHz, DMSO-d_6) δ in ppm: 170.66, 165.18, 137.99, 131.36, 129.93, 129.07, 128.60, 128.15, 127.20, 126.40, 123.16 (q, J = 287.7 Hz), 84.15 (q, J = 27.0 Hz), 74.21, 55.30, 52.01, 34.32, 27.31, 17.15

(*2R,3R*)-**4**-(*S*)-MTPA (**20**):

^{1}H-NMR (400 MHz, DMSO-d_6) δ 7.48 (s, 5H), 7.30 – 7.08 (m, 5H), 5.26 (p, ^{3}J = 6.4 Hz, 1H), 3.33 (s, 3H), 2.91 (ddd, ^{2}J = 10.8 Hz, ^{3}J = 6.9 Hz, ^{3}J = 5.0 Hz, 1H), 2.77 (dd, ^{2}J = 13.9 Hz, ^{3}J = 4.8 Hz, 1H), 2.64 (dd, ^{2}J = 13.6 Hz, ^{3}J = 10.8 Hz, 1H), 1.42 (d, ^{3}J = 6.4 Hz, 3H), 1.07 (s, 9H)

^{13}C-NMR (101 MHz, DMSO-d_6) δ in ppm: 170.35, 165.09, 138.08, 131.32, 129.91, 128.98, 128.63, 128.14, 127.13, 126.34, 123.16 (q, J_{C-F} = 287.7 Hz), 84.15 (q, J_{C-F} = 27.0 Hz), 80.25, 74.04, 55.15, 51.87, 33.94, 27.26, 17.22

(*2R,3S*)-**5**-(*S*)-MTPA (**21**):

^{1}H-NMR (400 MHz, DMSO-d_6) δ in ppm: 7.59 – 7.34 (m, 5H), 5.36 (p, ^{3}J = 6.5 Hz, 1H), 4.09 (dq, ^{3}J = 10.8 Hz, ^{3}J = 7.1 Hz, 1H), 3.99 (dq, ^{3}J = 10.9 Hz, ^{3}J = 7.1 Hz, 1H), 2.59 (dd, ^{3}J = 8.1 Hz, ^{3}J = 6.8 Hz, 1H), 2.00 – 1.83 (m, 1H), 1.27 (d, ^{3}J = 6.4 Hz, 3H), 1.12 (t, ^{3}J = 7.1 Hz, 3H), 0.96 (d, ^{3}J = 6.8 Hz, 3H), 0.87 (d, ^{3}J = 6.7 Hz, 3H)

^{13}C-NMR (101 MHz, DMSO-d_6) δ in ppm: 171.42, 165.07, 131.36, 129.91, 128.59, 127.15, 123.14 (q, $^{1}J_{C-F}$ = 288 Hz), 84.15 (q, $^{2}J_{C-F}$ = 27 Hz), 72.46, 60.04, 55.18, 54.99, 27.11, 20.17, 19.51, 15.60, 13.92

(*2S,3R*)-**5**-(*S*)-MTPA (**22**):

^{1}H-NMR (400 MHz, DMSO-d_6) δ 7.53 – 7.44 (m, 5H), 5.37 – 5.27 (m, 1H), 4.06 (dq, ^{3}J = 10.8 Hz, ^{3}J = 7.1 Hz, 1H), 3.94 (dq, ^{3}J = 10.8 Hz, ^{3}J = 7.1 Hz, 1H), 3.49 (s, 3H), 2.57 – 2.51 (m, 1H), 1.78 – 1.62 (m, 1H), 1.35 (d, ^{3}J = 6.3 Hz, 3H), 1.10 (t, ^{3}J = 7.1 Hz, 3H), 0.87 (d, ^{3}J = 6.8 Hz, 3H), 0.78 (d, ^{3}J = 6.7 Hz, 3H)

^{13}C-NMR (101 MHz, DMSO-d_6) δ in ppm: 171.16, 165.06, 131.48, 129.88, 128.57, 126.92, 123.14 (q, $^{1}J_{C-F}$ = 288 Hz), 84.14 (q, $^{2}J_{C-F}$ = 27 Hz), 72.23, 60.01, 55.28, 55.01, 26.78, 20.30, 18.93, 16.43, 13.95

(*2S,3S*)-**6**-(*S*)-MTPA (**23**):

^{1}H-NMR (400 MHz, DMSO-d_6) δ in ppm: 7.54 – 7.39 (m, 7H), 5.33 (dq, ^{3}J = 8.0 Hz, ^{3}J = 6.2 Hz, 1H), 3.46 (s, 3H), 2.38 (dd, ^{3}J = 8.2 Hz, ^{3}J = 6.1 Hz, 1H), 2.05 – 1.88 (m, 1H), 1.35 (s, 9H), 1.25 (d, ^{3}J = 6.3 Hz, 3H), 0.97 (d, ^{3}J = 6.9 Hz, 3H), 0.87 (d, ^{3}J = 6.7 Hz, 3H)

^{13}C-NMR (101 MHz, DMSO-d_6) δ in ppm: 170.48, 165.26, 131.40, 129.90, 128.56, 127.19, 123.14 (q, $^{1}J_{C-F}$ = 288 Hz), 84.14 (q, $^{2}J_{C-F}$ = 27 Hz), 80.47, 72.76, 56.15, 55.20, 27.66, 26.56, 20.95, 18.08, 17.06

(*2R,3R*)-**6**-(*S*)-MTPA (**24**):

^{1}H-NMR (400 MHz, DMSO-d_6) δ in ppm: 7.71 – 7.28 (m, 5H), 5.33 – 5.25 (m, 1H), 3.33 (s, 3H), 2.38 – 2.31 (m, 1H), 1.90 – 1.79 (m, 1H), 1.33 (d, 3H)[1], 1.29 (s, 9H), 0.90 (d, ^{3}J = 6.8 Hz, 3H), 0.82 (d, ^{3}J = 6.7 Hz, 3H)

^{13}C-NMR (101 MHz, DMSO-d_6) δ in ppm: 170.31, 165.14, 131.31, 129.88, 128.58, 127.10, 123.14 (q, $^{1}J_{C-F}$ = 288 Hz), 84.14 (q, $^{2}J_{C-F}$ = 27 Hz), 80.27, 72.59, 56.26, 55.08, 27.59, 26.37, 20.75, 18.39, 17.25

[1] superimposed with the singlet of *tert*-butylester

Table 9
Chemical shifts of γ-CH_3 groups of MTPA-Esters **13**-**24**.

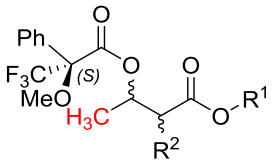

MTPA Ester	R^1	R^2	δ (γ-CH_3) [ppm]	Δδ (γ-CH_3) [ppm]
13	Et	Ph	1.25	0.05
14			1.30	
15	Et	Ph	1.00	0.10
16			1.10	
17	Et	Bn	1.30	0.09
18			1.39	
19	*t*Bu	Bn	1.34	0.08
20			1.42	
21	Et	iPr	1.27	0.08
22			1.35	
23	*t*Bu	iPr	1.25	0.08
24			1.33	

Supplementary material

Supplementary data to this article are available.

Declaration of Competing Interest

The authors declare that they have no known competing financial interests or personal relationships that could have appeared to influence the work reported in this paper.

Acknowledgments

This research has been funded by the European Social Fund (ESF, project no. 100310513) and the Free State of Saxony (grant 100316181 for Christian Trapp). In addition, we would like to thank the members of the project group *BioPlatZ* HSZG.

Supplementary materials

Supplementary material associated with this article can be found, in the online version, at doi:10.1016/j.mcat.2021.111578.

References

[1] J.M. Takacs, M.R. Jaber, A.S. Vellekoop, Preparation of Chiral Oxazolidin-2-ones and Vicinal Amino Alcohols, J. Org. Chem. 63 (1998) 2742–2748.
[2] M.J. Miller, Hydroxamate approach to the synthesis of .beta.-lactam antibiotics, Acc. Chem. Res. 19 (2002) 49–56.
[3] a) D. Kalaitzakis, I. Smonou, Chemoenzymatic Synthesis of Stegobinone and Stegobiol, Components of the Natural Sex Pheromone of the Drugstore Beetle (Stegobium paniceum L.), Eur. J. Org. Chem. 2012 (2012) 43–46;
b) J.-F. Zheng, H.-Q. Lan, R.-F. Yang, Q.-L. Peng, Z.-H. Xiao, S.-C. Tuo, K.-Z. Hu, Y.-G. Xiang, Z. Wei, Z. Zhang, P.-Q. Huang, Asymmetric Syntheses of the Sex Pheromones of Pine Sawflies, Their Homologs and Stereoisomers, Helv. Chim. Acta 95 (2012) 1799–1808;
c) K. Mori, Synthesis of optically active pheromones, Tetrahedron 45 (1989) 3233–3298.
[4] a) M. Bertau, M. Bürli, E. Hungerbühler, P. Wagner, A novel highly stereoselective synthesis of chiral 5- and 4,5-substituted 2-oxazolidinones, Tetrahedron: Asymmetry 12 (2001) 2103–2107;
b) E. Didier, B. Loubinoux, G.H. Ramos Tombo, G. Rihs, Chemo-enzymatic synthesis of 1,2- and 1,3- amino-alcohols and their use in the enantioselective reduction of acetophenone and anti-acetophenone oxime methyl ether with borane, Tetrahedron 47 (1991) 4941–4958;
c) A.K. Ghosh, H. Cho, M. Onishi, Asymmetric alkylations and aldol reactions: (1S,2R)-2-aminocyclopentan-1-ol derived new chiral auxiliary, Tetrahedron: Asymmetry 8 (1997) 821–824;
d) A. Varga, V. Zaharia, M. Nógrádi, L. Poppe, Chemoenzymatic synthesis of both enantiomers of 3-hydroxy- and 3-amino-3-phenylpropanoic acid, Tetrahedron: Asymmetry 24 (2013) 1389–1394.
[5] a) R. Bhuniya, T. Mahapatra, S. Nanda, Klebsiellapneumoniae (NBRC 3319) Mediated Asymmetric Reduction of α-Substituted β-Oxo Esters and Its Application to the Enantioiselective Synthesis of Small-Ring Carbocycle Derivatives, Eur. J.

Org. Chem. 2012 (2012) 1597–1602;
b) D. Zhu, C. Mukherjee, J.D. Rozzell, S. Kambourakis, L. Hua, A recombinant ketoreductase tool-box. Assessing the substrate selectivity and stereoselectivity toward the reduction of β-ketoesters, Tetrahedron 62 (2006) 901–905.
[6] M.M. Victor, J.E. Uchôa, V.B. Riatto, First use of cactus and cushcush as biocatalysts in the enantioselective reduction of β -keto esters, Industrial Crops and Products 96 (2017) 126–131.
[7] V. Stepankova, S. Bidmanova, T. Koudelakova, Z. Prokop, R. Chaloupkova, J. Damborsky, Strategies for Stabilization of Enzymes in Organic Solvents, ACS Catalysis 3 (2013) 2823–2836.
[8] a) M.Á. Fernández-Ibáñez, B. Maciá, A.J. Minnaard, B.L. Feringa, Katalytische enantioselektive Reformatsky-Reaktionen mit Aldehyden, Angew. Chem. 120 (2008) 1337–1339;
b) I. Kholod, O. Vallat, A.-M. Buciumas, A. Neels, R. Neier, Synthetic Strategies for the Synthesis and Transformation of Substituted Pyrrolinones as Advanced Intermediates for Rhazinilam Analogues, Eur. J. Org. Chem. 2014 (2014) 7865–7877;
c) P.V. Ramachandran, P.B. Chanda, Enantioselective synthesis of anti- and syn-beta-hydroxy-alpha-phenyl carboxylates via boron-mediated asymmetric aldol reaction, Chem Commun (Camb) 49 (2013) 3152–3154.
[9] R. Noyori, T. Ikeda, T. Ohkuma, M. Widhalm, M. Kitamura, H. Takaya, S. Akutagawa, N. Sayo, T. Saito, T. Taketomi, H. Kumobayashi, Stereoselective hydrogenation via dynamic kinetic resolution, J. Am. Chem. Soc. 111 (1989) 9134–9135.
[10] a) T. Nakata, Y. Tani, M. Hatozaki, T. Oishi, Stereoselective reduction of .ALPHA.-methyl-.BETA.-hydroxy ketones with zinc borohydride, Chem. Pharm. Bull. (Tokyo) 32 (1984) 1411–1415;
b) T. Nakata, T. Oishi, Stereoselective reduction of β-keto esters with zinc borohydride. stereoselective synthesis of -3-hydroxy-2-alkylpropionates, Tetrahedron Lett 21 (1980) 1641–1644.
[11] E. Marcantoni, S. Alessandrini, M. Malavolta, G. Bartoli, M.C. Bellucci, L. Sambri, R. Dalpozzo, Reversed Stereochemical Control in the Presence of CeCl3and TiCl4in the Lewis Acid Mediated Reduction of α-Alkyl-β-keto Esters by Metal Hydrides. A General Methodology for the Diastereoselective Synthesis ofsyn- andanti-α-Alkyl-β-hydroxy Esters, J. Org. Chem. 64 (1999) 1986–1992.
[12] T. Mandai, T. Oshitari, M. Susowake, Lipase-catalyzed Transesterification of Methyl 2-Substituted 3-Hydroxy-4-pentenoates and its Synthetic Application to the Taxol Side Chain, Synlett (2002) 1665–1668, https://doi.org/10.1055/s-2002-34247.
[13] G. Gu, J. Lu, O. Yu, J. Wen, Q. Yin, X. Zhang, Enantioselective and Diastereoselective Ir-Catalyzed Hydrogenation of alpha-Substituted beta-Ketoesters via Dynamic Kinetic Resolution, Org. Lett. 20 (2018) 1888–1892.
[14] N. Ran, L. Zhao, Z. Chen, J. Tao, Recent applications of biocatalysis in developing green chemistry for chemical synthesis at the industrial scale, Green Chem 10 (2008) 361–372.
[15] S. Sen, J.E. Puskas, Green polymer chemistry: enzyme catalysis for polymer functionalization, Molecules 20 (2015) 9358–9379.
[16] L.E. Meyer, J. von Langermann, U. Kragl, Recent developments in biocatalysis in multiphasic ionic liquid reaction systems, Biophys Rev 10 (2018) 901–910.
[17] A.L.B. Dias, P. dos Santos, J. Martínez, Supercritical CO2 technology applied to the production of flavor ester compounds through lipase-catalyzed reaction: A review, Journal of CO2 Utilization 23 (2018) 159–178.
[18] E. Durand, J. Lecomte, P. Villeneuve, Deep eutectic solvents: Synthesis, application, and focus on lipase-catalyzed reactions, Eur. J. Lipid Sci. Technol. 115 (2013) 379–385.
[19] A. Fishman, M. Eroshov, S.S. Dee-Noor, J. van Mil, U. Cogan, R. Effenberger, A two-step enzymatic resolution process for large-scale production of (S)- and (R)-ethyl-3-hydroxybutyrate, Biotechnol. Bioeng. 74 (2001) 256–263.
[20] C. Trapp, C. Herrmann, C. Drewniok, D. Greif, M. Hofrichter, Diastereoselective reduction of selected α-substituted β-keto esters and the assignment of the relative configuration by 1H-NMR spectroscopy, Current Organocatalysis (2021) 8.
[21] a)Novozymes in *Immobilized lipases for biocatalysis*, Vol. 2016. b) C. Ortiz, M. L. Ferreira, O. Barbosa, J.C.S. dos Santos, R.C. Rodrigues, Á. Berenguer-Murcia, L. E. Briand, R. Fernandez-Lafuente, Novozym 435: the "perfect" lipase immobilized biocatalyst? Catalysis Science & Technology 9 (2019) 2380–2420.
[22] C. Laane, S. Boeren, K. Vos, C. Veeger, Rules for optimization of biocatalysis in organic solvents, Biotechnol. Bioeng. 30 (1987) 81–87.
[23] a) Z.Q. Duan, W. Du, D.H. Liu, The solvent influence on the positional selectivity of Novozym 435 during 1,3-diolein synthesis by esterification, Bioresour. Technol. 101 (2010) 2568–2571;
b) G.D. Yadav, S. Devendran, Lipase catalyzed synthesis of cinnamyl acetate via transesterification in non-aqueous medium, Process Biochem 47 (2012) 496–502.
[24] E.M. Anderson, K.M. Larsson, O. Kirk, One Biocatalyst–Many Applications: The Use of Candida Antarctica B-Lipase in Organic Synthesis, Biocatal. Biotransform. 16 (1997) 181–204.
[25] J. Ottosson, K. Hult, Influence of acyl chain length on the enantioselectivity of Candida antarctica lipase B and its thermodynamic components in kinetic resolution of sec-alcohols, J. Mol. Catal. B: Enzym. 11 (2001) 1025–1028.
[26] C. Orrenius, F. Hbffner, D. Rotticci, N. öhrner, T. Norin, K. Hult, Chiral Recognition Of Alcohol Enantiomers In Acyl Transfer Reactions Catalysed ByCandida AntarcticaLipase B, Biocatal. Biotransform. 16 (2009) 1–15.
[27] D.T. Lai, C.J. O'Connor, Studies on synthesis of short chain alkyl esters catalyzed by goat pregastric lipase, J. Mol. Catal. B: Enzym. 6 (1999) 411–420.
[28] A. Zaidi, J.L. Gainer, G. Carta, A. Mrani, T. Kadiri, Y. Belarbi, A. Mir, Esterification of fatty acids using nylon-immobilized lipase in n-hexane: kinetic parameters and chain-length effects, J. Biotechnol. 93 (2002) 209–216.
[29] P. Borowiecki, D. Paprocki, A. Dudzik, J. Plenkiewicz, Chemoenzymatic Synthesis of Proxyphylline Enantiomers, J. Org. Chem. 81 (2016) 380–395.
[30] L.F. García-Alles, V. Gotor, Alcohol inhibition and specificity studies of lipase B fromCandida antarctica in organic solvents, Biotechnol. Bioeng. 59 (1998) 163–170.
[31] a) J.A. Dale, H.S. Mosher, Nuclear magnetic resonance enantiomer regents. Configurational correlations via nuclear magnetic resonance chemical shifts of diastereomeric mandelate, O-methylmandelate, and .alpha.-methoxy-.alpha.-trifluoromethylphenylacetate (MTPA) esters, J. Am. Chem. Soc. 95 (1973) 512–519;
b) I. Ohtani, T. Kusumi, Y. Kashman, H. Kakisawa, High-field FT NMR application of Mosher's method. The absolute configurations of marine terpenoids, J. Am. Chem. Soc. 113 (1991) 4092–4096.
[32] a) L.E. Janes, R.J. Kazlauskas, Empirical rules for the enantiopreference of lipase from Aspergillus niger toward secondary alcohols and carboxylic acids, especially α-amino acids, Tetrahedron: Asymmetry 8 (1997) 3719–3733;
b) M. Cygler, P. Grochulski, R.J. Kazlauskas, J.D. Schrag, F. Bouthillier, B. Rubin, A.N. Serreqi, A.K. Gupta, A Structural Basis for the Chiral Preferences of Lipases, J. Am. Chem. Soc. 116 (1994) 3180–3186.
[33] S. Hünig, P. Kreitmeier, G. Märkl, J. Sauer, Arbeitsmethoden in der organischen Chemie, Verlag Lehmanns, 2006.
[34] O. Trott, A.J. Olson, AutoDock Vina: improving the speed and accuracy of docking with a new scoring function, efficient optimization, and multithreading, J. Comput. Chem. 31 (2010) 455–461.
[35] G.M. Morris, R. Huey, W. Lindstrom, M.F. Sanner, R.K. Belew, D.S. Goodsell, A. J. Olson, AutoDock4 and AutoDockTools4: Automated docking with selective receptor flexibility, J. Comput. Chem. 30 (2009) 2785–2791.
[36] B. Stauch, S.J. Fisher, M. Cianci, Open and closed states of Candida antarctica lipase B: protonation and the mechanism of interfacial activation, J. Lipid Res. 56 (2015) 2348–2358.
[37] L. Schrodinger, The PyMOL molecular graphics system, Version 1 (2010), 0.
[38] A.R. Aguillón, M.N. Avelar, L.E. Gotardo, S.P. de Souza, R.A.C. Leão, I. Itabaiana, L. S.M. Miranda, R.O.M.A. de Souza, Immobilized lipase screening towards continuous-flow kinetic resolution of (±)-1,2-propanediol, Molecular Catalysis 467 (2019) 128–134.